INFLUENCE OF COPPER SUBSTITUTION ON ELECTRICAL PROPERTIES OF Mg-Cu-Zn FERRITE

Su Su Tha[1], Hsan Htoo[2]

Abstract

Magnesium copper zinc ferrites with the general formula $Mg_{0.5}Cu_xZn_{0.5-x}Fe_2O_4$(x=0, 0.1, 0.2, 0.3, 0.4, 0.5) were prepared by mixing stoichiometric proportions of magnesium, copper, zinc and ferrite nitrates with calculated amount of citric acid. Before mixing, four raw samples were checked by XRD to confirm these samples are pure or not. Four raw samples, magnesium nitrates: copper nitrate: zinc nitrates: ferric nitrates ($Mg(NO_3)_2.6H_2O$, $Cu(NO_3)_2.6H_2O$, $Zn(NO_3)_2.6H_2O$, $Fe(NO_3)_3.9H_2O$) were mixed with citric acid ($C_6H_8O_7$) in different ratios in the beaker and stirring at 70°C until to get viscous gel. And then the samples were calcined at 800˚C for 2 hr. The structural analysis, crystallize size and surface morphology investigation of as prepared samples were studied by Powder X-ray Diffractometer (XRD) and Scanning Electron Microscopy (SEM) techniques. The temperature dependent resistivity of Mg-Cu-Zn ferrites were analysis in various concentration of copper.

Keywords: *XRD, SEM* and *Resistivity*

Introduction

With the rapid development of mobile communication and information technology, small, inexpensive, high performance electronic devices are in high demand. Recently, we have witnessed the rapid development of surface mounting devices (SMD) using multilayer chip inductors (MLCI), which utilize alternating coats of ferrite and electrical paste, followed by co-firing. High temperature co-firing (normally higher than 1000 °C) causes a decrease in inductance due to the interfacial reaction (via diffusion) between ferrite and silver, usually use as electrode material. This interfacial reaction can be suppressed by co-firing at a temperature lower than the melting point of Ag (approximately 960 °C). Therefore, low temperature sintering is of great importance to suppress the interfacial diffusion. Whereas, Mg-Cu-Zn ferrites are more suitable to overcome these problems. The citrate precursor method is a promising technique for the synthesis of certain technical ceramics. Since all the reactants are solutions, they can be uniformly mixed on an atomic or molecular level, and the amount of the reactants can be accurately controlled. This wet chemical method has unique advantages over conventional sintering processes in terms of obtaining nanoparticles that can be densified easily at lower temperature. The aim of this work is to present a novel and economical method of preparation of Mg-Cu-Zn ferrite by the citrate precursor method in order to achieve sintering at lower temperatures.

The spinel ferrite (MFe_2O_4, M = a divalent cation) belongs to and important class of magnetic materials, because of their remarkable magnetic properties particularly in radio frequency region, physical flexibility high electrical resistivity, mechanical hardness and chemical stability. For its excellent properties, more attention was paid to Mg-Cu-Zn ferrite, which is mainly applied in electrical devices and in catalysis.

Materials and Methods

Experimental Procedure

The samples of $MgCuZnFe_2O_4$ mixed ferrite were prepared by mixing magnesium nitrate, zinc nitrate, copper nitrate and ferric nitrates with calculated amount of citric acid. Four raw

[1] PhD Candidate, Lecturer, Department of Physics, Mawlamyine University.
[2] Dr., Associate Professor, Department of Physics, Kalay University.

samples were checked by XRD to confirm these samples are pure or not. The different ratios of the six mixtures were staring at 70˚C to get viscos gel. And then the samples were pre sintering at 70 ˚C until to get dry powder. Then the powder samples were sintering at 800 ˚C for 2 hours. During heating the crucible, the crystal water was gradually vaporized. When a crucible temperature was reached to the critical temperature, large amounts of foams produced with appearance of spark at one corner which spread through the mass in the container. Flow diagram of the sample preparation procedure of magnesium copper zinc ferrite is given in Figure 1.

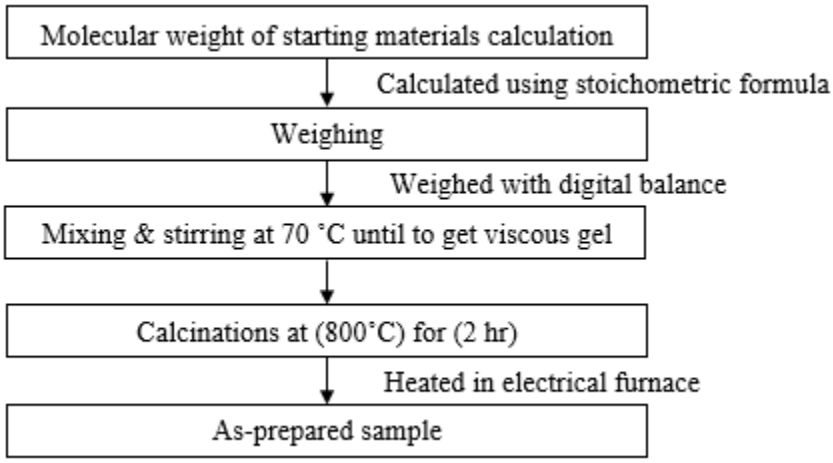

Figure 1 Flow diagram of the sample preparation procedure of magnesium copper zinc ferrite

Results and Discussion

X Ray Diffraction Measurement

X-ray diffraction is the most widely used and least ambiguous method for the precise determination of the positions of atoms in molecules and solids. In X-ray diffraction (XRD) measurement, a beam of X-ray directed on a crystalline material may experience diffraction (constructive interference) as a result of its interaction with a series of atomic plane according to Bragg's law. Since interplanar spacing is a function of the miller indices, lattice gathering much useful information relating the crystal structure. The value of interplanar spacing, d_{hkl} is function of miller indices (h, k and l) as well as the lattice parameter. The lattice parameters of the unit cell of the cubic represent:

$$\frac{1}{d^2} = \left[\frac{h^2 + k^2 + l^2}{a^2}\right]$$

where d = interplanar spacing
a = lattice parameter
(h k l) = Miller indices

The crystallite size can be measured as following Debye-Scherrer formula.

$$D = \frac{k\,\lambda}{B\,\mathbf{cos}\,\theta}$$

Where, D = Crystallite size (Å)
λ = The wavelength of X-ray use (1.5405 Å)
B = Full Width Half Maximum of dominant peak (radians)
θ = Angle of diffraction (radians)
k = scherrer constant

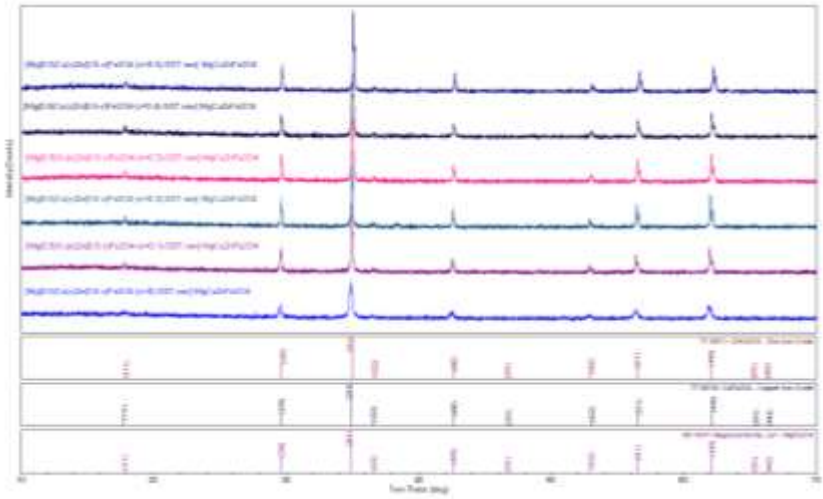

Figure 2 Peak comparisons of XRD patterns for $Mg_{(0.5)}Cu_{(x)}Zn_{(0.5-x)}Fe_2O_4$ samples

Table 1 Comparisons of lattice parameters and crystallite sizes for $Mg_{(0.5)}Cu_{(x)}Zn_{(0.5-x)}Fe_2O_4$ sample

x	Lattice (a) (Å)	Crystalize Size (nm)
0.00	8.5489	20.73
0.10	8.6126	47.19
0.20	8.5334	44.68
0.30	8.5632	44.61
0.40	8.5483	29.63
0.50	8.5192	37.26

Surface Morphology Investigation using SEM

Scanning electron microscopy (SEM) as shown in the following figure is a widely spread technique, used in materials and biological sciences as well as in industry. Modern scanning electron microscopies combine high spatial resolution imaging and analysis capabilities with easy to handle hardware and user- friendly computer-based interface. The scanning electron microscope (SEM) is a type of electron microscope that creates various images by focusing a high energy beam of electrons onto the surface of a sample and detecting signals from the interaction of the incident electrons with the sample's surface. The type of signals gathered in a SEM varies and can include secondary electrons, characteristic X-rays, and back scattered electrons. The focused electron beam is scanned across the sample surface, generating different signals. The richness in signal opens up the possibility to investigate a wide range of materials properties. The two most commonly used signals for imaging in the SEM are secondary electrons and back scattered electrons.

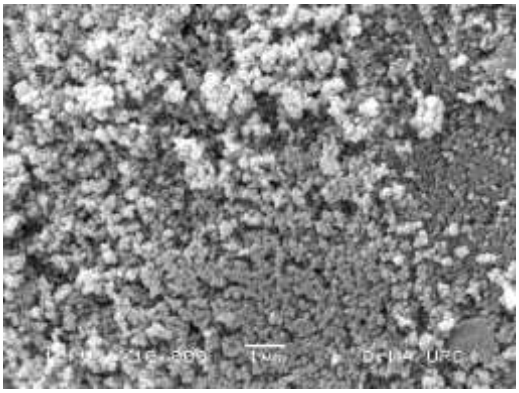

Figure 3 SEM image of $Mg_{(0.5)}Zn_{(0.5)}Fe_2O_4$ (800°) sample

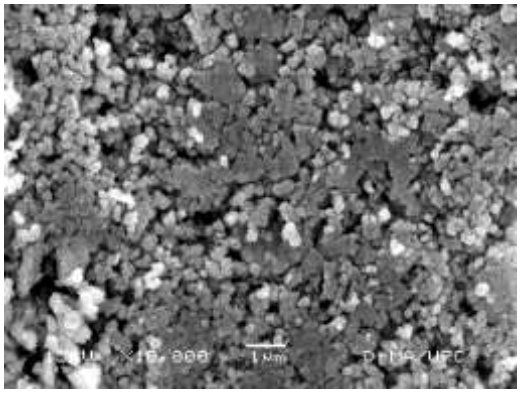

Figure 4 SEM image of $Mg_{(0.5)}Cu_{(0.1)}Zn_{(0.4)}Fe_2O_4$ (800°C) sample

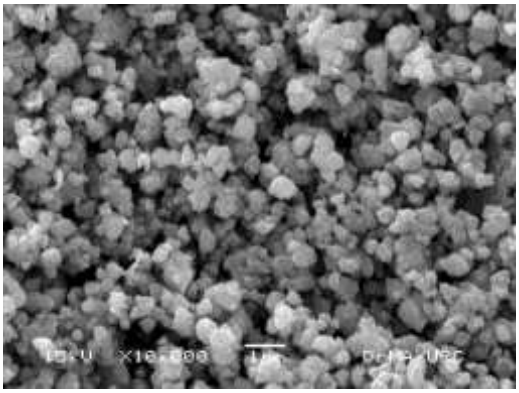

Figure 5 SEM image of $Mg_{(0.5)}Cu_{(0.2)}Zn_{(0.3)}Fe_2O_4$ (800°C) sample

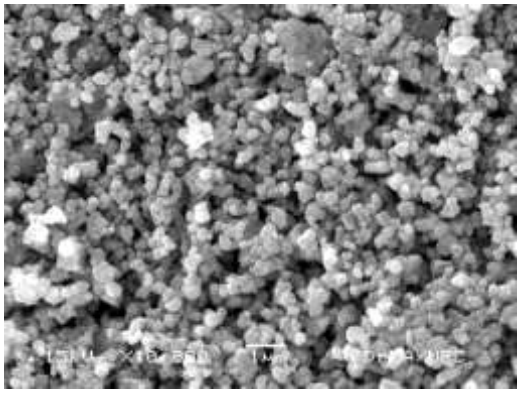

Figure 6 SEM image of $g_{(0.5)}Cu_{(0.3)}Zn_{(0.2)}Fe_2O_4$ (800°C) sample

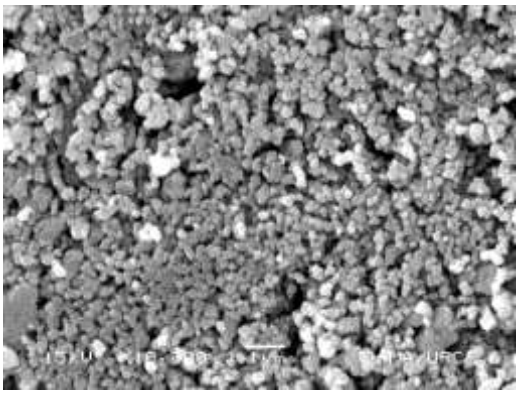

Figure 7 SEM image of $Mg_{(0.5)}Cu_{(0.4)}Zn_{(0.1)}Fe_2O_4$ (800°C) sample

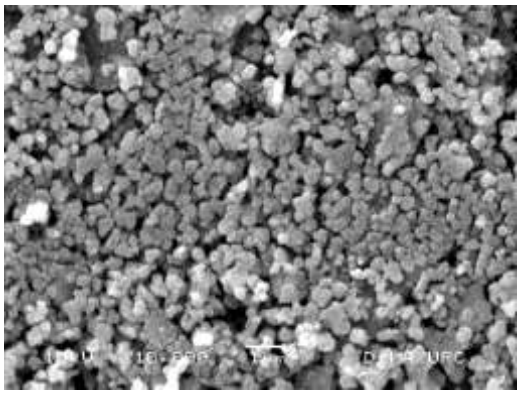

Figure 8 SEM image of $Mg_{(0.5)}Cu_{(0.5)}Fe_2O_4$ (800°C) sample

Table 2 Comparisons of grain size for $Mg_{(0.5)}Cu_{(x)}Zn_{(0.5-x)}Fe_2O_4$ sample

x	Grain size (μm)
0.0	0.186
0.1	0.199
0.2	0.205
0.3	0.209
0.4	0.232
0.5	0.269

The microstructure and morphology have an important role in determining the magnetic and electric transport properties and those were examined by a high resolution scanning electron microscope. These studied for the materials are essential in order to understand the relationship between their processing parameters as well as the behavior when used in practical applications. The morphology of the as prepared sample was achieved by using SEM technique. SEM images with same magnification for the $Mg_{(0.5)}Cu_{(x)}Zn_{(0.5-x)}Fe_2O_4$ samples are given in Figure 3 to 8. These images display formation of spongy and homogeneous material. Average grain size was determined using Image J software. The surface morphology of the $Mg_{(0.5)}Cu_{(x)}Zn_{(0.5-x)}Fe_2O_4$ (calcined at 800˚C)sample as seen from the SEM photographs consists of grain size varying from (0.186) to (0.269) μm and it was generally uniform in grain size. There can be concluded that the grain size increases with increasing the molar ratio of Cu substitution.

Temperature Dependent Electrical Resistivity

The measurements on electrical resistivity were performed on the final sintered pellets. An Aplab LCR meter (MT-4080D) assisted by a temperature controller was used to observe the temperature dependent resistivity. In the first step, the dimension of the sample of the sample was measured by using slide caliper. Then, the sample was sandwiched between two copper plates that serve as two electrodes. To ensure better electrical contact, silver paste was evenly applied on both surfaces of the sample.

The sample was placed in a sample holder that was immersed in a heating chamber surrounded by asbestos. Each copper plate was brought into contact with copper rod from the chamber. Thermal conducting mica shield was used between the sample and the chamber to have a good thermal conductivity and to protect from electrical conduction. The resistances were measured over a temperature range from 300K to 700K at interval of 20K by using Aplab LCR meter. The J-type thermocouple was inserted near the sample to record its temperature. Temperature of the specimen was kept constant by a controller. Figure illustrates sample holder for resistivity measurement. The resistivity of each sample was calculated by using the following relation:

$$\rho = \frac{RA}{l}$$

Where *l* is the thickness of the sample in cm, A is the area of the electrode in contact with sample (πr^2) in cm^2 and R is the resistance in Ω. The relationship between resistivity and temperature can be expressed as:

$$\rho = \rho_0 \exp(E_a / k_b T)$$

Where, ρ_0 is the resistivity extrapolated to T, E_a is the activation energy, k_B is the Boltzmann constant and T is the absolute temperature. This equation can be converted in the form of linear equation. From the plot of log (ρ) versus temperature (1000/T), the activation energy is calculated. The electrical resistivity is found that the resistivity of all the samples decrease with increase in temperature, and then the resistivity becomes stable above temperature 400K. Kumar et al, studied electrical properties of a series of copper substituted Mg-Zn ferrites with the compositional formula $Mg_{(0.5)}Cu_{(x)}Zn_{(0.5-x)}Fe_2O_4$. Experimental results that they satisfied, showed that DC electrical resistivity decreases with increase of temperature ensuring the semiconducting nature of the ferrites "Kumar et al., 2014". The decrease in resistivity with temperature may be attributed to the increase in drift mobility of the charge carriers.

Figure 9 shows the variation of the electrical resistivity of Cu concentration of $Mg_{(0.5)}Cu_{(x)}Zn_{(0.5-x)}Fe_2O_4$. It has been observed that room temperature resistivity values of bulk

samples are seen to vary between 1.0×10^{7}ohm-cm to 8.7×10^{7} ohm-cm. The resistivity values of $Mg_{(0.5)}Cu_{(x)}Zn_{(0.5-x)}Fe_2O_4$ increases with increase in concentration of copper x=0.1 to x=0.3. The resistivity values of copper substituted $Mg_{(0.5)}Cu_{(x)}Zn_{(0.5-x)}Fe_2O_4$decrease with increase in concentration of copper x=0.3 to x=0.5. The resistivity values of $Mg_{(0.5)}Cu_{(x)}Zn_{(0.5-x)}Fe_2O_4$ decreases as increase in the temperature range between 300K to 400K and then the resistivity will becomes stable above temperature 400K in Figure 9(a) to (e).

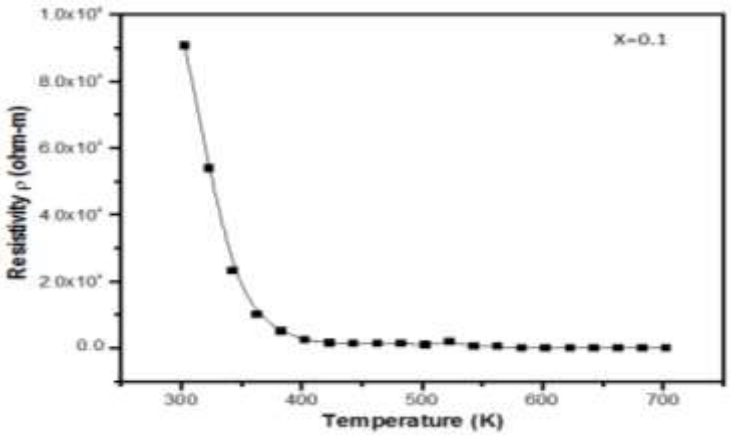

Figure 9 (a) Temperature dependent resistivity curves for $Mg_{(0.5)}Cu_{(x)}Zn_{(0.5-x)}Fe_2O_4$with Cu content (x=0.1)

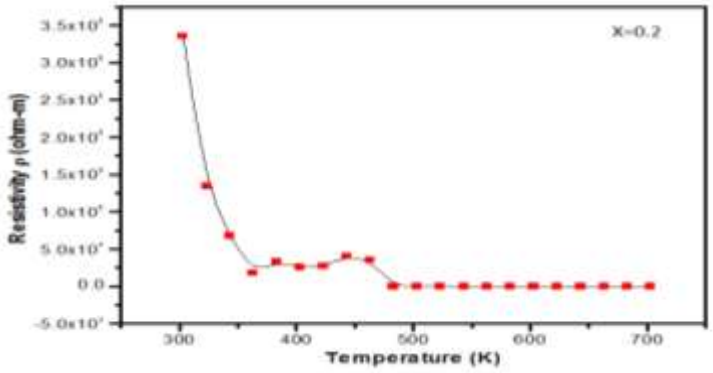

Figure 9 (b) Temperature dependent resistivity curves for $Mg_{(0.5)}Cu_{(x)}Zn_{(0.5-x)}Fe_2O_4$ with Cu content (x=0.2)

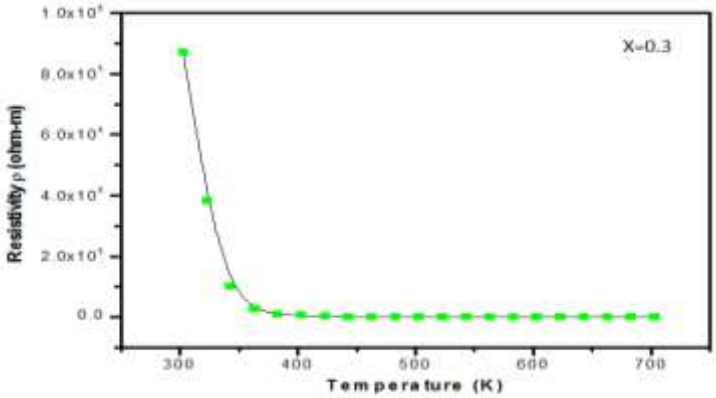

Figure 9 (c) Temperature dependent resistivity curves for $Mg_{(0.5)}Cu_{(x)}Zn_{(0.5-x)}Fe_2O_4$ with Cu content (x=0.3)

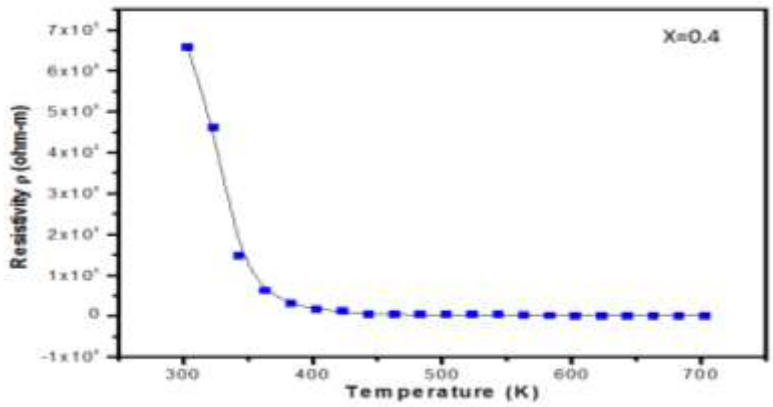

Figure 9 (d) Temperature dependent resistivity curves for $Mg_{(0.5)}Cu_{(x)}Zn_{(0.5-x)}Fe_2O_4$ with Cu content (x=0.4)

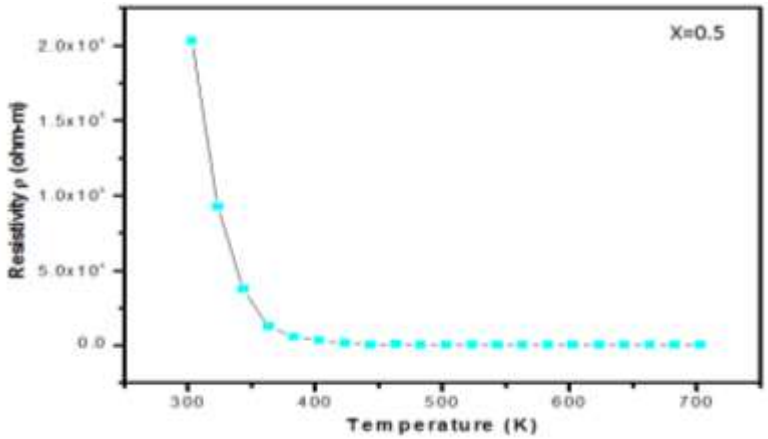

Figure 9 (e) Temperature dependent resistivity curves for $Mg_{(0.5)}Cu_{(x)}Zn_{(0.5-x)}Fe_2O_4$ with Cu content (x=0.5)

Table 3 The variation of resistivity with different Cu concentration at 373K

Cu Concentration	R (Ω)	Resistivity (Ωm)
0.1	1151383.04	282592.00
0.2	6562009.80	1610560.00
0.3	19073807.13	4681418.00
0.4	7862017.54	1929630.00
0.5	2298976.93	564254.00

Conclusion

Magnesium copper zinc ferrites $Mg_{(0.5)}Cu_{(x)}Zn_{(0.5-x)}Fe_2O_4$ has been determined in various ratios as (x=0.0, 0.1, 0.2, 0.3. 0.4, 0.5). The preparation method for the investigated system is sol gel method. According the XRD results, the crystallize sizes of ferrite samples were calculated to be 20.73, 47.19, 44.68, 44.61, 29.63 and 37.26 nm at the various ratios of (x=0.0, 0.1, 0.2, 0.3, 0.4, 0.5) respectively. And lattice parameters are nearly the same as 8.6Å. It was clear that the crystallize size of ferrite sample with mixed ratio of (x=0.0) (or) $Mg_{(0.5)}Zn_{(0.5)}Fe_2O_4$ was smallest crystallite size about 20.73nm among all samples. But the crystallize size of ferrite sample with mixed ratio of (x=0.4) (or) $Mg_{(0.5)}Cu_{(0.4)}Zn_{(0.1)}Fe_2O_4$ was smallest crystallize size about 29.63 nm

among four mixed samples. X-ray diffraction analysis clearly revealed that all the ferrites have the structure cubic spinel. According of SEM results, grain size of as prepared samples are varying from (0.186) to (0.269) μm and it was generally uniform in grain size. It can be concluded that the grain size increases with increasing the molar ratio of Cu substitution.

The resistivity values of $Mg_{(0.5)}Cu_{(x)}Zn_{(0.5-x)}Fe_2O_4$ decreases as increase in the temperature range between 300K to 400K and then the resistivity will be stable above 400K as shown in figures.

Acknowledgements

The authors are grateful to the Department of Physics and Universities' Research Centre, University of Yangon, for the supports with research facilities and also. The authors are also grateful to the colleagues from the Department of Physics, Mawlamyine University for their encouragement to this work.

References

Bondyopadhyay, A. K. (2010). "Nano Materials" (New Delhi: New Age)

Kittle, C, (2005). "Introduction to Solid State Physics", (New York: Wiley)

Nakamura, T. (2017). "Journal of Magnetism and Magnetic Material". Mater. 168, 285-291.

Pillai S. O. (2006). "Solid State Physics" (New Delhi: New Age)

Qi, X., Zhou, J., Yue, Z., Gui, Z., Li, L. (2002). "Journal of Magnetism and Magnetic Material". Mater. 251, 316-322.

Zhang, H., Li, L., Wu, P., Zhou, J., Ma, Z. & Gui, Z. (2000). "Journal of Magnetism and Magnetic Materials". Mat. Res. Bull. 352, 207-2215.

Zhang, H., Ma, Z., Zhou, J., Yue, Z., Li, L. & Gui, Z. (2000). "Journal of Magnetism and Magnetic Materials". Mater. 213, 304-308.